Available online at www.sciencedirect.com
SCIENCE DIRECT®
Chemical Physics Letters 393 (2004) 488–492
CHEMICAL PHYSICS LETTERS
www.elsevier.com/locate/cplett

Quantum coding and decoding in multi-level adiabatic passage schemes

Petr Král *, Moshe Shapiro

Department of Chemical Physics, Perlman Bldg., Weizmann Institute of Science, 76100 Rehovot, Israel
Department of Chemistry and Physics, University of British Columbia, Vancouver, Canada V6T1Z1

Received 7 May 2004; in final form 14 June 2004

Abstract

We present quantum schemes that can code/decode information by optical adiabatic passage processes. In a *quantum decoder*, information encoded on N levels (quNit), with population amplitudes of M possible phases, is processed by transferring their population optically to (predominantly) *one* of L final levels. In this two-photon adiabatic passage, N intermediate levels are resonantly coupled 'one-to-one' to N initial states and 'one-to-all' to L final states. A *quantum encoder* works in the opposite way. We discuss practical implementation of the suggested schemes in manifolds of vibrational states of the Na_2 dimer.

1. Introduction

Practical realization of many challenging problems in quantum computation [1], quantum communication [2] and use of quantum devices [3,4] is limited by decoherence effects [5]. Various approaches have been suggested to overcome this problem, like using of robust codes [6,7] or decay-free states [8]. It is thus of interest to search systems that can perform general unitary operations [9] and convert quantum information between different codes.

In this work, we present new schemes that can efficiently code and decode quantum information, when applied in molecular systems. They are based on robust two-photon adiabatic passage techniques [10–12], which are generalized to include *many* initial, intermediate and final states. This step allows selective addressing of many final states, according to a priori *unknown* initial superposition states. Analogous multi-level schemes can be used in preparation of vibrational wave packets in molecular dimers [13], in chiral purification of 'racemic' mixtures of enantiomers [14] or in control of isomerization of Jahn–Teller molecules [15].

2. Quantum decoder

In the *quantum decoder*, which is shown in Fig. 1, information is encoded on N initial energy levels, $|i\rangle_A$ ($i=1,\ldots,N$), with M distinct phases of their population amplitudes, that form 'discrete' quNit states [16]. The initial $|i\rangle_A$ states are resonantly coupled one-to-one to N *intermediate* $|i\rangle_B$ states, by a 'pump' pulse of Ω_{ii}^{AB} Rabi frequencies. These states are in turn resonantly coupled one-to-all to a (larger) set of final $|k\rangle_C$ states ($k=1-L$), by a 'dump' pulse of Ω_{ik}^{BC} Rabi frequencies. In this two-photon multi-path adiabatic passage, we use a 'counter-intuitive' pulse ordering [10–12], in which the 'dump' (D) pulse precedes the 'pump' (P) pulse. Decoding is realized by passing the population on the N initial $|i\rangle_A$ states to predominantly *one* of the L final $|k\rangle_C$ states.

* Correpsonding author. Fax: +972-8-9344123.
E-mail address: kral@weizmann.ac.il (P. Král).

0009-2614/$ - see front matter © 2004 Elsevier B.V. All rights reserved.
doi:10.1016/j.cplett.2004.06.091

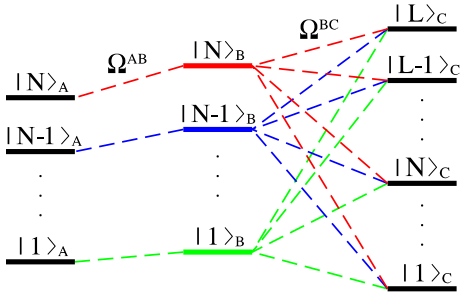

Fig. 1. Scheme of the quantum adiabatic de/encoder. In a quantum decoder, the information is initially encoded in the M phases of population amplitudes of the $|1-N\rangle_A$ states. Its decoding is realized by transferring all the population through the intermediate $|1-N\rangle_B$ states to predominantly *one* of the final $|1-L\rangle_C$ states ($L>N$). Quantum encoder works in the opposite way: it transfers the population from a single $|1-L\rangle_C$ state to all the $|1-L\rangle_A$ states and fixes their M phases.

The coupling is mediated by multimode electric fields

$$E_{P(D)}(t) = R_e \sum_{k,l} E^{AB(BC)}_{k,l}(t) e^{-i\omega^{AB(BC)}_{k,l} t}. \quad (1)$$

Thus, $\Omega^{AB(BC)}_{kl}(t) \equiv \mu^{AB(BC)}_{k,l} E^{AB(BC)}_{k,l}(t) \equiv O^{AB(BC)}_{k,l} f_{P(D)}(t)$ are the Rabi frequencies, where we use the electric-dipole matrix-elements $\mu^{AB(BC)}_{k,l}$ between the $|k\rangle_{A(B)}$ and $|l\rangle_{B(C)}$ states, and $0<f_{P(D)}(t)<1$ are the common envelopes of the dump and pump pulses.

The total Hamiltonian, in the rotating waves approximation and neglecting off-resonance terms, is ($\hbar = 1$)

$$\begin{aligned} H = & \sum_{\ell=1}^{2N+L} \omega_\ell \mid \ell\rangle\langle\ell \mid \\ & + \sum_{i=1}^{N} \left[\Omega^{AB}_{ii}(t) e^{-i\omega^{AB}_{i,i} t} \mid i\rangle_B\langle i|_A + h.c.\right] \\ & + \sum_{i=1}^{N}\sum_{k=1}^{L} \left[\Omega^{BC}_{ki}(t) e^{-i\omega^{BC}_{k,i} t} \mid k\rangle_C\langle i|_B + h.c.\right]. \end{aligned} \quad (2)$$

In the first sum, ℓ goes over all states of the system, with energies ω_ℓ. The second term represents the one-to-one resonant coupling of the initial states to the intermediate states, by the pump pulse whose frequency components are $\omega^{AB}_{i,i} \equiv \omega_{i_B} - \omega_{i_A}$. The third term represents the one-to-all resonant coupling of the intermediate states to the final states, by the dump pulse with frequency components $\omega^{BC}_{k,i} \equiv \omega_{k_C} - \omega_{i_B}$. We assume that the level energies are such that only the described couplings are resonant and parasitic effects due to non-resonant neighboring couplings can be neglected [13].

We expand the system wave function in the material states as, $|\psi(t)\rangle = \sum_k c_j(t) e^{-i\omega_k t}|k\rangle$. The column vector of slow varying coefficients $\mathbf{c} = (c_1, c_2, \ldots)$ is a solution of the matrix-Schrödinger equation $\dot{\mathbf{c}}(t) = -iH(t)\cdot\mathbf{c}(t)$. The effective time-dependent Hamiltonian is

$$H(t) = \begin{bmatrix} \mathbf{0} & \mathbf{H}^{AB} & \mathbf{0} \\ \mathbf{H}^{AB\dagger} & \mathbf{0} & \mathbf{H}^{BC} \\ \mathbf{0} & \mathbf{H}^{BC\dagger} & \mathbf{0} \end{bmatrix}, \quad (3)$$

where $\mathbf{H}^{AB}_{i,j} = \Omega^{AB}_{ii}\delta_{ij}$ is a diagonal and $\mathbf{H}^{BC}_{ik} = \Omega^{BC}_{ik}$ a full matrix. We can find that $H(t)$ has $2N+L$ eigenvalues, of which at most $2N$ are nonzero, $\lambda_{1,\ldots,2N}(t) \neq 0$, and the rest L are zero, $\lambda_{2N+1,\ldots,2N+L}=0$, so they correspond to 'null' states. Re-defining the basis as $e^{-i\omega_\ell t}|\ell\rangle \to |\ell\rangle$, we can check from $H\cdot\mathbf{d}_k = 0$ ($k = 1-L$) that these states are characterized by the time-dependent vectors,

$$\begin{aligned} \mathbf{d}_1 &= \left(\Omega^{BC}_{11}/\Omega^{AB}_{11}, \ldots, \Omega^{BC}_{N1}/\Omega^{AB}_{NN}, 0, \ldots, 0, -1, 0, \ldots, 0\right), \\ \mathbf{d}_2 &= \left(\Omega^{BC}_{12}/\Omega^{AB}_{11}, \ldots, \Omega^{BC}_{N2}/\Omega^{AB}_{NN}, 0, \ldots, 0, 0, -1, \ldots, 0\right), \\ &\vdots \\ \mathbf{d}_L &= \left(\Omega^{BC}_{1L}/\Omega^{AB}_{11}, \ldots, \Omega^{BC}_{NL}/\Omega^{AB}_{NN}, 0, \ldots, 0, 0, 0, \ldots, -1\right). \end{aligned} \quad (4)$$

In order to simplify the analysis, we can assume, without loss of generality [13], that $\Omega^{AB}_{11} = \Omega^{AB}_{22} = \ldots = \Omega^{AB}_{NN} = \Omega^{AB}$. Then, the first N coefficients in the $\mathbf{d}_k(t)$ null states are *solely* determined by the dump vectors $\mathbf{\Omega}_{Dk} = (\Omega^{BC}_{1k}, \Omega^{BC}_{2k}, \ldots, \Omega^{BC}_{Nk})$. Moreover, the $\mathbf{d}_k(t)$ states correlate one-to-one with the $|1-L\rangle_C$ final states. Thus, if we manage to initially populate only *one* of the $\mathbf{d}_k(t)$ states, adiabatic following would exclusively pass this population to a *single* final $|k\rangle_C$ state, in the end of the process, so the decoding process would be perfect.

In reality, the initial population of the $|1-N\rangle_A$ states splits among the ($k = 1-L$) dark states, according to the squared projections, $p_k \propto |\mathbf{c}_0\cdot\mathbf{\Omega}_{Dk}|^2$, of the vector of initial coefficients $\mathbf{c}_0 = (c_1, c_2, \ldots, c_N)$ on the dump vectors $\mathbf{\Omega}_{Dk}$. Analogous relation determines the fraction of population transferred through a *single* intermediate level [13], by many *pump* Rabi frequencies. Therefore, we can maximize the population p_i, transferred to the chosen (decoded) $|i\rangle_C$ state, by using $\mathbf{\Omega}_{Di} \propto \boldsymbol{c}_0$. At the same time, parasitic transfers to other $|k\rangle_C$ ($k \neq i$) states could be minimized if the $\mathbf{\Omega}_{Dk}$ and $\mathbf{\Omega}_{Di}$ vectors are orthogonal, $\mathbf{\Omega}_{Dk}\cdot\mathbf{\Omega}_{Di} \approx 0$. The first condition is easy to meet, while the last cannot be fully realized if $N < L$. This is because, we cannot orthogonalize *all* the L vectors, $\mathbf{\Omega}_{Dk}$, in a $N(<L)$ dimensional space. Only if $N = L$, their components can be chosen such that the L dark states are orthogonal one to another, in the form given in Eq. (4), and the transfers to the final $|k\rangle_C$ states are complete *and* exclusive. Very good coding/decoding machines can still be realized, unless $N \ll L$.

As an example, we can examine the transfer of number information stored in $M = 2$ phases of the coefficients of N equally populated initial levels $|i\rangle_A$. In this 'binary-phase' coding the binary number (0,0,...,0), i.e., $0\cdot 2^0 + 0\cdot 2^1 + \cdots + 0\cdot 2^N = 0$, is represented by the amplitude $\mathbf{c}_1 = (1,1,\ldots,1)$ of the $|i\rangle_A$ states, the binary number

(1,0,...,0), i.e., $1\cdot 2^0+0\cdot 2^1+\cdots+0\cdot 2^N=1$, by $\mathbf{c}_2=(-1,1,\ldots,1)$, and so on. Because quantum states are known up to an overall phase, we can encode in this manner on N levels only 2^{N-1} numbers.

As mentioned above, the decoding can be optimized by aligning Rabi vectors $\mathbf{\Omega}_{\mathrm{D}k}$, which dump population to the $|k\rangle_{\mathrm{C}}$ states, with the related $\mathbf{c}_k$ vectors of encoded coefficients, $\mathbf{\Omega}_{\mathrm{D}k}\propto \mathbf{c}_k$. Accordingly, the $|1\rangle_{\mathrm{C}}$ state is coupled to the intermediate $|1-N\rangle_{\mathrm{B}}$ states by the vector of Rabi amplitudes $O_{\mathrm{D}1}=(1,1,\ldots,1)=\mathbf{c}_1$, the $|2\rangle_{\mathrm{C}}$ state by $O_{\mathrm{D}2}=(-1,1,\ldots,1)=\mathbf{c}_2$, and so on.

In Fig. 2, we present the quantum decoder. The magnitudes of all the Rabi frequencies are $|O_{ij}|=30/\tau$, where $f_{\mathrm{D}(\mathrm{P})}(t)=\exp[-(t-t_{\mathrm{D}(\mathrm{P})})^2/\tau^2]$ and $t_{\mathrm{P}}-t_{\mathrm{D}}=2\tau$. The system *decodes* each of the binary-phase stored number by transferring the population of the initial superposition state, representing this number, to predominantly *one* of the (16) final $|k\rangle_{\mathrm{C}}$ eigenstates. The degree of exclusivity of the transfer is such that 5 other final states end up with 2.78 times less population, while the remaining 10 states being considerably less populated.

We can obtain *analytically* the populations p_k of the final $|k\rangle_{\mathrm{C}}$ states, that are proportional to the squared scalar products, $p_k\propto|\mathbf{c}_0\cdot\mathbf{\Omega}_{\mathrm{D}k}|^2$, of the *encoded initial vector* $\mathbf{c}_0=(c_1,c_2,\ldots,c_5)$ with the dump Rabi vectors $\mathbf{\Omega}_{\mathrm{D}k}$. For example, by encoding the first 'hexagonal' level, $\mathbf{c}_0=(1,1,1,1,1)$, and taking into account that $O_{\mathrm{D}1}=(1,1,1,1,1)$ and $O_{\mathrm{D}2}=(-1,1,1,1,1)$, we obtain that $p_1\propto|\mathbf{c}_0\cdot O_{\mathrm{D}1}|^2=25$ and $p_2\propto|\mathbf{c}_0\cdot O_{\mathrm{D}2}|^2=9$, so that $p_1/p_2=|5/3|^2\approx 2.78$, as in Fig. 2. From the scalar products $\mathbf{c}_0\cdot O_{\mathrm{D}1-16}$, we can get all the probabilities, p_{1-16}; five of them are $\frac{9}{25}p_1$ and 10 are $\frac{1}{25}p_1$. Thus, from the normalization factor $n=1+5(9/25)+10(1/25)=3.2$, we obtain $p_1=1/n=0.3125$, determining the populations p_k in all the cases.

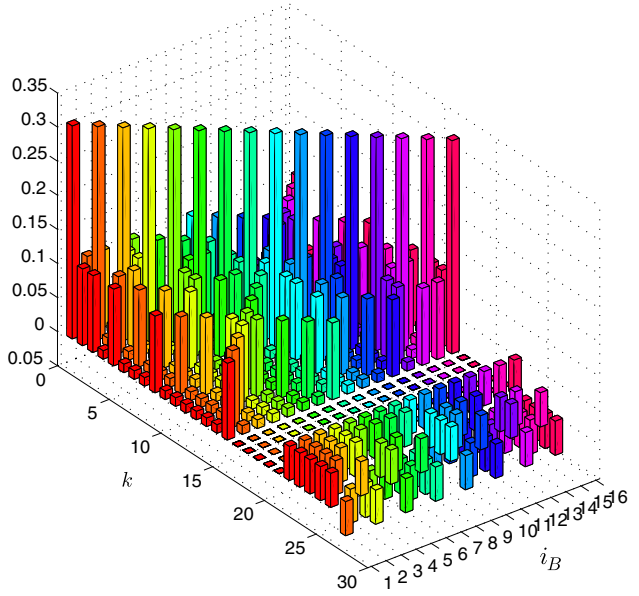

Fig. 2. The results of the quantum decoder. In the back we see the p_k ($k=1$–16) populations of the $2^{N-1}=16$ final levels, transferred from the $N=5$ initial states ($k=22$–26), shown up front. The intermediate states ($k=17$–21), in the mid-region, are unpopulated. The c_k amplitudes of the five initial states are depicted by bars, 0.05 in height (instead of the correct $1/\sqrt{5}$ values). As we decode different binary-phase stored numbers $i_{\mathrm{B}}-1$, the maximum (31%) of the transferred population moves from one final level to the next. Other final levels are at least 2.78 times less populated.

Let us now generalize the decoding devices. We can increase the density of coding [17], by using the initial 'discrete' quNit states, with amplitudes of M *different* phases of the $\exp(\mathrm{i}2\pi j/M)$ roots of the identity. Therefore, a system with N initial levels and information stored in M possible phases can be prepared in M^{N-1} states and transferred to the same number of final levels.

In Tables 1 and 2, we present for selected systems the maximal population $p_{\max}$ and the ratio $r=p_{\max}/p_{\mathrm{next}}$ of the maximal and next to maximal populations on the final states. We have calculated them as in Fig. 2, by numerically enumerating all the possible states, and confirming the results by dynamical simulations. The ratio r, which determines the decoding selectivity, can be considered to be good if $r>2$, that is for systems above or on the diagonal in Tables 1 and 2, given by $N=6$ and $M=4$. Clearly the decoding is better the closer the number of the N initial/intermediate and M^{N-1} final states is, i.e. the smaller N and M are. The efficiency of en/decoding in these systems could approach that in standard quantum gates [1], if the pulses are tailored to the processed quantum information.

Since relaxation is neglected, the (unitary) evolution is invertible. Thus the population can be transferred back by the same set of pulses using a time-reversed dump–pump pulse sequence. In practice, we could detect the final decoded state by monitoring its fluorescence to some lower lying state, but after the measurement the coherence is largely lost. Of a large practical interest is the question, whether we can use

Table 1
The (maximal) population $p_{\max}$ of the final decoded state

$p_{\max}$	$N=2$	$N=3$	$N=4$	$N=5$	$N=6$
$M=2$	1	0.75	0.5	0.313	0.188
$M=3$	0.666	0.333	0.148	0.062	0.025
$M=4$	0.5	0.188	0.063	0.020	0.006

Here, N is the number of levels and M the number of phases used.

Table 2
The ratio $r=p_{\max}/p_{\mathrm{next}}$ of the maximal and next to maximal populations of the final decoded states

r	$N=2$	$N=3$	$N=4$	$N=5$	$N=6$
$M=2$	∞	9	4	2.78	2.25
$M=3$	4	3	2.29	1.92	1.71
$M=4$	2	1.8	1.6	1.47	1.38

the inverted pulse sequence for encoding numbers into the phases, by starting out just with a *single* populated 'hexadecimal' level.

3. Quantum encoder

In Fig. 3, we display the results of this quantum encoding. In each run, we initially populate *one* of the (16) 'hexadecimal' $|k\rangle_C$ levels, shown in Fig. 2, and evolve the system by the time reversed pulse sequence. In the front of Fig. 3, we see the binary-phase coded amplitudes of the (5) $|i\rangle_A$ levels. In the back, we show populations left on the 'hexadecimal' levels. In contrast to the quantum converter scheme, the coding here is *perfect*, since we obtain the correct phases of the $|i\rangle_A$ states. However the transfer is far from *complete*, since about 50% of the population is left on the initial 'hexadecimal' level and 15% is scattered to other 'hexadecimal' levels. This transfer from many to fewer levels is hampered by 'bottle-necks', with a portion of the population being channeled back to the original states, as discussed below. The transfer could be increased to [1] ≈100%, if we use different pulses [13], since the 16 levels are orthogonal. But we might not be able to keep them *the same for all the situations*.

As mentioned above, when $N<L$, the L null states can not be made orthogonal one to another, in the form shown in Eq. (4). Nevertheless, it is still possible to have

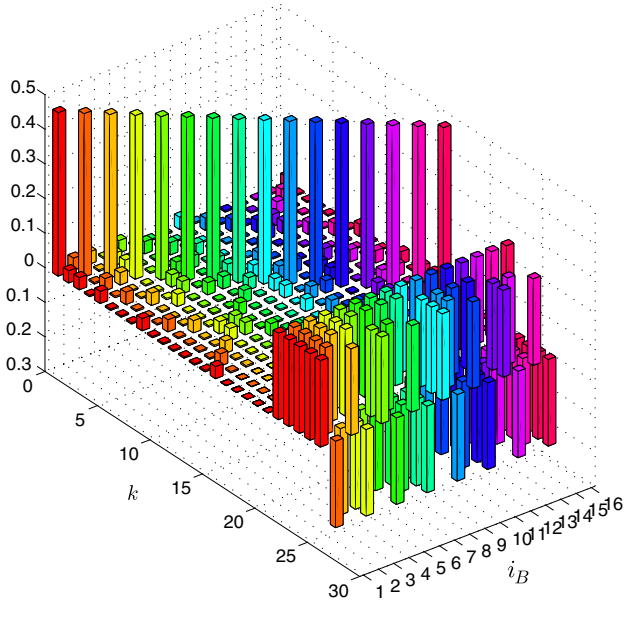

Fig. 3. The results of the quantum encoder, depicted as in Fig. 2. The correctly coded binary-phase amplitudes c_k of the $N=5$ final levels are shown in front (in true height). The populations p_k left on the initial 16 states are shown in the back. In each case about 50% of the initial 'hexadecimal' population is transferred: 31% are transferred to the correctly binary-phase coded levels and 19% goes to other states.

N of these dark states linearly independent in the subspace of the first N coefficients. We can thus combine, and orthogonalize, the L dark states in such a way, that N of the new states would have nonzero first N coefficients, while $L-N$ would have them zero,

$$\mathbf{D}_l(t) = \sum_j \alpha_{lj}\mathbf{d}_j(t), (\mathbf{D}_{l=(N+1)-L})_{1-2N} = 0. \quad (5)$$

We thus end with N null states, for which population transfer is *complete*, called 'mixed null states' (MNS), and $L-N$ null states, called 'initial null states' (INS) [13], for which *no population* transfer is possible, since they do not couple to the $|1-N\rangle_A$ (final) states.

We illustrate this behavior in a four-level system, with levels $|1\rangle$ and $|2\rangle$ coupled to level $|3\rangle$ by the pump pulse $\mathbf{\Omega}_P=(\Omega_{13},\Omega_{23})\propto(1,1)$, where we assume $\Omega_{13}=\Omega_{23}$, and level $|3\rangle$ coupled to level $|4\rangle$ by the dump pulse Ω_{34}. From Eq. (4), we obtain the two null states $\mathbf{d}_1=(-1,0,0,\Omega_{13}/\Omega_{34},)$ and $\mathbf{d}_2=(0,-1,0,\Omega_{23}/\Omega_{34})$. These states can be combined to form the MNS, $\mathbf{d}_1+\mathbf{d}_2=(-1,-1,0,(\Omega_{13}+\Omega_{23})/\Omega_{34})$, and the INS, $\mathbf{d}_1-\mathbf{d}_2=(-1,1,0,0)$. Likewise, the initially populated state $|1\rangle$ can be written as $|1\rangle=0.5|S\rangle+0.5|A\rangle$, where $|S\rangle=|1\rangle+|2\rangle$ *parallel* and $|A\rangle=|1\rangle-|2\rangle$ is *orthogonal* to $\mathbf{\Omega}_P$. As a result of the action of the $\mathbf{\Omega}_P$ and Ω_{34} pulses, the $|S\rangle$ state, initially correlated to the MNS, becomes depopulated ($p_4=0.5$), while the population of the $|A\rangle$ state, $p_A=0.5$, correlated to the INS, remains intact.

This system can be extended in a chain-like manner to the case in which levels $|1\rangle$, $|2\rangle$, $|3\rangle$ are coupled to levels $|4\rangle$, $|5\rangle$ by the pump pulses $\Omega_{14}=\Omega_{24}=\Omega_{25}=\Omega_{35}$, with levels $|4\rangle$ and $|5\rangle$ coupled to $|6\rangle$ and $|7\rangle$ by the dump pulse $\Omega_{46}=\Omega_{57}$. If any of the $|1\rangle-|3\rangle$ states is initially populated, 2/3 of the population is transferred and 1/3 remains intact. This can be seen by resolving the initially populated level as, $|2\rangle=(|2\rangle-|1\rangle-|3\rangle)+|1\rangle+|3\rangle$. From Eq. (4), we find that one MNS correlates level $|1\rangle$ to $|6\rangle$, the other correlates level $|3\rangle$ to $|7\rangle$, while the INS is *always* correlated to $|2\rangle-|1\rangle-|3\rangle$. By following this chain of 'frustrated' transfers, we obtain that the total population transferred in each case is 1/2, 2/3, 3/4, ..., i.e., the ratio of the number of intermediate levels and the number of initial levels. This 'quantum reflection law' is rather general, as we show below.

We can examine analogously the MNS and INS states in Fig. 3. We initially consider only the $|1-4\rangle_C$ states, with $|1\rangle_C$ initially populated. Their coupling vectors are $\mathbf{c}_1=(1,1,1,1,1)$, $\mathbf{c}_2=(-1,1,1,1,1)$, $\mathbf{c}_3=(1,-1,1,1,1)$ and $\mathbf{c}_4=(-1,-1,1,1,1)$. Then, $\mathbf{c}_4$ is linearly dependent on the other three vectors, $\mathbf{c}_4=\mathbf{c}_2+\mathbf{c}_3-\mathbf{c}_1$, and the reflected populations are $p_{1-4}=1/16$. If we wish to encode the vector $\mathbf{c}_5=(1,1,-1,1,1)$, instead of $\mathbf{c}_4$, the $\mathbf{c}_{2,3,5}$ vectors would be linearly independent on $\mathbf{c}_1$. Therefore, no INS correlating to the $|1\rangle_C$ state can be formed, and the population is fully transferred. When we also add

the $|8\rangle_C$ state, with $\mathbf{c}_8=(-1,-1,-1,1,1)=\mathbf{c}_2+\mathbf{c}_3+\mathbf{c}_5-2\mathbf{c}_1$, the INS correlates *more* with the $|1\rangle_C$ state and the reflected populations are $p_2=p_3=p_5=p_8=p_1/4$. By adding more and more states, we finally match Fig. 3, where all these cases interfere and give a large reflected population, mostly left on the $|1\rangle_C$ state.

We can find the probability P_{tran} of transfer from a *single* (decoded) level to *all* the (encoded) levels in general systems. Then, among the M^{N-1} null states, N are MNS and $M^{N-1}-N$ are INS. In accordance with the above quantum reflection law, we might expect that $P_{\text{tran}}=N/M^{N-1}$. Dynamical simulations fully confirm this fact. Surprisingly, these values are *identical* with those in Table 1, i.e. $P_{tran}=p_{\max}$. The same holds for the probability of transfer to the 'incorrectly decoded' levels and back; in the last case, we need to project the transferred population amplitudes on the *initially* encoded amplitudes. These adiabatically driven systems thus behave as 'passive' multi-channel elements, with the same transfer probabilities in both directions.

4. Practical realization

We can apply the above de/coding schemes in manifolds of molecular vibrational states, such as those found in the Na_2 dimer [13]. The initial vibrational wave packet, $|\Psi(0)\rangle=\sum_{v=1}^{M}c_v^0|X^1\Sigma_g^+,v\rangle$, is sitting on the *ground* electronic state $X^1\Sigma_g^+$ of the Na_2 molecule [18], where $c_v^0=\pm1$ are chosen according to the encoded number. It could be prepared in simpler multi-level adiabatic schemes [13]. The $|X^1\Sigma_g^+,v=1-M\rangle$ vibrational states are coupled one-to-one to the intermediate $|A^1\Sigma_u^+,v'=1-M\rangle$ vibrational states, sitting on the *excited* electronic state $X^1\Sigma_g^+$. These are then coupled one-to-all to the $|X^1\Sigma_g^+,v=(M+1)-(M+L)\rangle$ vibrational states. Since the vibrations are not harmonic, the resonant transitions should not interfere one with another, if the pulses are long enough [13].

The resonant electric field components $E_{v',v}(t)e^{-i\omega_{v',v}t}$, introduced in Eq. (1), have the amplitudes $E^{AB}_{v',v}(t)=f_D(t)\delta_{v',v}C/\mu_{v',v}(\delta_{v',v}=1,0$ if $v'=v$ resp. $v'\neq v)$ and $E^{BC}_{v',v}(t)=f_P(t)Cc^e_{v',v}/\mu_{v',v}$, where the transition-dipole matrix elements are [19,20] $\mu_{v',v}\equiv\langle A^1\Sigma_u^+,v\prime|\hat{\epsilon}\cdot\mu|X^1\Sigma_g^+,v\rangle$. For $c^e_{v',v}=\pm1$, chosen according to the decoding structure, the adiabaticity can be satisfied for $C=30/\tau=1$ ps^{-1} and $f_{D(P)}(t)$ as in Fig. 2. With this choice, we obtain the above Rabi frequencies, since $\Omega^{AB}_{v',v}(t)=\mu_{v',v}E^{AB}_{v',v}(t)=f_D(t)C(v'=v)$ and $\Omega^{CD}_{v',v}(t)=\mu_{v',v}E^{CD}_{v',v}(t)=f_P(t)Cc^e_{v',v}$. This shows that small molecules, such as the Na_2 dimer, could be used to realize the suggested de/coding schemes.

Acknowledgements

We thank I. Thanopulos for many useful discussions. This project was supported by the Minerva Foundation, GIF, the EU IHP program HPRN-CT-1999-00129, the Office of Naval Research, USA.

References

[1] M.A. Nielsen, I.L. Chuang, Quantum Computation and Quantum Information, Cambridge University Press, Cambridge, 2000.
[2] L.-M. Duan, M.D. Lukin, J.I. Cirac, P. Zoller, Nature. 414 (2001) 413.
[3] Y.S. Weinstein, M.A. Pravia, E.M. Fortunato, S. Lloyd, D.G. Cory, Phys. Rev. Lett. 86 (2001) 1889.
[4] L.M.K. Vandersypen et al., Nature. 414 (2001) 883.
[5] G.M. Palma, K.-A. Suominen, A.K. Ekert, Proc. Roy. Soc. London Sect. A 452 (1996) 567.
[6] A.R. Calderbank, P.W. Shor, Phys. Rev. A 54 (1996) 1098.
[7] D.A. Lidar, I.L. Chuang, K.B. Whaley, Phys. Rev. Lett. 81 (1998) 2594.
[8] M. Shapiro, P. Brumer, Phys. Rev. A 66 (2002) 052308.
[9] S. Franke-Arnold, E. Andersson, S.M. Barnett, S. Stenholm, Phys. Rev. A 63 (2001) 052301;
Z. Kis, F. Renzoni, Phys. Rev. A 65 (2002) 032318.
[10] A. Kuhn et al., J. Chem. Phys. 96 (1992) 4215;
K. Bergmann, H. Theuer, B.W. Shore, Rev. Mod. Phys. 70 (1998) 1003.
[11] J. Oreg, F.T. Hioe, J.H. Eberly, Phys. Rev. A 29 (1984) 690.
[12] M.N. Kobrak, S.A. Rice, Phys. Rev. A 57 (1998) 1158;
M.N. Kobrak, S.A. Rice, J. Chem. Phys. 109 (1998) 1;
M.N. Kobrak, S.A. Rice, Phys. Rev. A 57 (1998) 2885.
[13] P. Král, M. Shapiro, Phys. Rev. A 65 (2002) 043413;
P. Král, Z. Amitay, M. Shapiro, Phys. Rev. Lett. 89 (2002) 063002.
[14] P. Král, M. Shapiro, Phys. Rev. Lett. 87 (2001) 183002;
P. Král, I. Thanopulos, M. Shapiro, D. Cohen, Phys. Rev. Lett. 90 (2003) 033001;
I. Thanopulos, P. Král, M. Shapiro, J. Chem. Phys. 119 (2003) 5105.
[15] I. Thanopulos, P. Král, M. Shapiro, Phys. Rev. Lett. 92 (2004) 11003.
[16] D. Kaszlikowski, P. Gnacinski, M. Zukowski, W. Miklaszewski, A. Zeilinger, Phys. Rev. Lett. 85 (2000) 4418.
[17] S.L. Braunstein, H.J. Kimble, Phys. Rev. A 61 (2000) 042302.
[18] D.G. Abrashkevich, I.Sh. Averbukh, M. Shapiro, J. Chem. Phys. 101 (1994) 9295.
[19] G. Herzberg, Molecular Spectra and Molecular Structure: I. Spectra of Diatomic Molecules, second ed., Van Nostrand, Princeton, 1950.
[20] W.J. Stevens, M.M. Hessel, P.J. Bertoncini, A.C. Wahl, J. Chem. Phys. 66 (1977) 1477.